Spin-lattice relaxation rate of a magnetic impuritiy in the spin degenerate Anderson model

J. W. M. Pinto and H. O. Frota Departamento de Física-ICE, Universidade Federal do Amazonas, 69077-000, Manaus-Am, Brazil

December 29, 2021

Abstract

The renormalization group formalism was applied to calculate the spinlattice relaxation rate T_1^{-1} of a well-defined magnetic moment in the neighborhood of a spin degenerate Anderson impurity. In the Kondo regime, T_1^{-1} in function of the temperature T presents a peak at the Kondo temperature T_k ; for $T \ll T_k$, the system behaves as a heavy Fermy liquid, with an enhanced density of states, which increases with the decreasing of the Kondo temperature; $T_1^{-1}T$ remains an universal function of T/Γ_k up to temperatures the order of $100\Gamma_k$, where Γ_k is the Kondo width; for temperatures lower then T_k , the spin relaxation rate, T_1^{-1} , is proportional to the magnetic susceptibility multiplied by the temperature, χT ; the peak of T_1^{-1} at the Kondo temperature decreases with the increasing of the distance between the Anderson impurity and the magnetic probe.

The authors would like to thank Ufam (the Amazonas Federal University) and CNPq/Brazil for the financial support.

1 Introduction

The one impurity spin degenerated Anderson model [1] has been studied by different many bodies techniques, such as Green Function, Renormalization Group, Bethe Ansatz, Quantum Monte Carlo and combination of Quantum Monte Carlo with the of Maximum Entropy method. The static and dynamic properties was obtained, such as specific heat, magnetic susceptibility, photoemission and nuclear magnetic resonance. The Electron Spin Resonance (ESR) of a probe with a well deffined magnetic moment added to that model remains to be better studied, which is the main point of the present work. This model has been useful to analyze the behavior of heavy fermions and intermediate valence compounds so that the calculation of the ESR can contribute to a better understanding of the experimental results of the ESR in those compounds. The ESR of a magnetic impurity embedded in a heavy fermion compounds results in an

enhancement in the Korringa rate [2]. However, the results for the intermediate valence compounds are controverted. Gambke at al [3] associated the reduction in the relaxation rate of Gd in CePd₃ to the intermediate valence state. On the other hand, Heirinch and Meyer [4] have observed the opposite phenomena in CeBe₁₃:Gd, as well Barberis at al [5] in CeIr₂:Nd and Rettori at al [6] in YbInCu₄:Gd. In the Anderson model the configuration of the Anderson ion can be changed continuously from doubly occupied to empty orbital, which allows us to analyze the effect of the Anderson impurity orbital occupation number on the ESR relaxation rate, from the doubly to the singly occupied orbital regimes, passing by the valence fluctuation regime.

In the present work we hve applied the numerical renormalization group (NRG) method of Wilson [7, 8, 9] to research the relaxation rate T_1^{-1} of a magnetic probe embedded in a host represented by the single impurity spin degenerate Anderson model. Originally Wilson discretized the conduction band defining the sequence $\varepsilon_j = D\Lambda^{-j}$ (where D is the half-width of the conduction band, $\Lambda > 1$ and j = 1, 2, 3...) as a discrete set of conduction states. The Anderson Hamiltonian is projected onto the basis formed by this set and the Anderson ion states and is diagonalized iteratively and the thermodynamic average over those discrete eigenvalues are smooth functions of temperature. The magnetic probe relaxation rate T_1^{-1} , however, in a consequence of the Fermi golden rule energy conservation, shows only discrete line transitions. To overcome this difficulty we discretize the conduction band by the sequence $\varepsilon_o = D$, $\varepsilon_i = D\Lambda^{-j-z}$, where z is a continuous parameter fixed arbitrarily inside intervals $(z^*, z^* + 1)$, with $z^* \in (0,1)$, as was done in references [10] and [11]. The Anderson Hamiltonian is projected onto the basis formed by the new set and the impurity states, and is diagonalized iteratively. Continuum spectra are obtained by averaging numerically the T_1^{-1} over z, at each temperature, in the range $z^* < z < z^* + 1$.

The present paper is organized as follows: Section II details the model and describes the relaxation rate; Section III develops the formalism to obtain the relaxation rate from the Fermi golden rule; Section IV shows the results and discussion of the relaxation rate, and Section V contains the conclusions.

2 The Model

The model is represented by the single impurity Anderson model H and a magnetic probe sitting at $\overrightarrow{R_p}$, interacting with the Anderson ion, sitting at $\overrightarrow{R_f}$, via the RKKY interaction H_x [12]. The single impurity Anderson model consists of the kinetic energy of the free electrons (H_{cond}) , the bound energy of the Anderson ion orbital (H_{orb}) and the hybridization of this orbital with the conduction band (H_{hib}) ,

$$H = H_{cond} + H_{orb} + H_{hib}. (1)$$

The Hamiltonian of the conduction electrons is written as

$$H_{cond} = \sum_{\overrightarrow{k},\mu} \varepsilon_{\overrightarrow{k}} c_{\overrightarrow{k},\mu}^{\dagger} c_{\overrightarrow{k},\mu}, \qquad (2)$$

where $c_{\vec{k}\mu}^{\dagger}(c_{\vec{k}\mu})$ creates (annihilates) an electron in the conduction band with energy $\varepsilon_{\vec{k}}$, spin μ and momentum \vec{k} , obeying the usual anticommutation relation $\left\{c_{\vec{k},\mu},c_{\vec{k'},\mu'}^{\dagger}\right\} = \delta\left(\vec{k}-\vec{k'}\right)\delta_{\mu\mu'}$. The second term in Eq. (1), corresponding to the Anderson ion orbital, is given by

$$H_{orb} = \sum_{\mu} \varepsilon_f c_{f,\mu}^{\dagger} c_{f,\mu} + U c_{f\uparrow}^{\dagger} c_{f\uparrow} c_{f\downarrow}^{\dagger} c_{f\downarrow}, \qquad (3)$$

where the operator $c_{f\mu}^{\dagger}(c_{f\mu})$, orthonormal to the operator $c_{\overrightarrow{k},\mu}^{\dagger}(c_{\overrightarrow{k},\mu})$ of the conduction band, creates (annihilates) an electron in the Anderson ion orbital (f) with energy ε_f and spin μ , and U is the Coulomb interaction between the electrons in that orbital. The Hamiltonian H_{hib} in Eq. (1) is written as

$$H_{hib} = V \sum_{\overrightarrow{k},\mu} \left(c_{\overrightarrow{k},\mu}^{\dagger} c_{f,\mu} + c_{f,\mu}^{\dagger} c_{\overrightarrow{k},\mu} \right), \tag{4}$$

where V is the hybridization interaction between the electrons of the f orbital and the conduction band electrons. For a moment, if we consider that there is no coupling between the Anderson ion orbital and the conduction electrons (V=0), this orbital may be empty $(n_f=c_{f\mu}^{\dagger}c_{f\mu}=0 \text{ and energy } 0)$, singly $(n_f=1 \text{ and energy } \epsilon_f)$ or doubly $(n_f=2 \text{ and energy } 2\epsilon_f+U)$ occupied orbital. The introduction of the interaction $V\neq 0$ allows transitions between those configurations at a rate $\Gamma=\pi\rho V^2$, via the conduction band, whose density of state is ρ . In this case the model can represent the intermediate valence $(|\Delta|<\Gamma)$ and the Kondo $(\Delta, -\epsilon_f\gg\Gamma)$ regimes, where $\Delta=\epsilon_f+U$ is the interconfigurational energy.

The interaction between the magnetic probe and the Anderson ion orbital (H_x) , that will be treated as a perturbation, is given by

$$H_x = -A \left[\Psi_{\uparrow}^{\dagger} \left(\overrightarrow{R_p} \right) \Psi_{\downarrow} \left(\overrightarrow{R_p} \right) \mathbf{I}_{-} + \Psi_{\downarrow}^{\dagger} \left(\overrightarrow{R_p} \right) \Psi_{\uparrow} \left(\overrightarrow{R_p} \right) \mathbf{I}_{+} \right], \tag{5}$$

where A is the coupling constant between the magnetic probe and the conduction electrons, and the field operator $\Psi^{\dagger}_{\uparrow}\left(\overrightarrow{R_p}\right)$ is written as

$$\Psi_{\mu}\left(\overrightarrow{R_{p}}\right) = \sum_{\overrightarrow{k}} e^{i\overrightarrow{k} \cdot \overrightarrow{R_{p}}} c_{\overrightarrow{k},\mu}, \tag{6}$$

which annihilates an electron in the Wannier state at the site of the magnetic probe $(\overrightarrow{R_p})$, and $\mathbf{I}_{-(+)}$ is the lowering (raising) spin operator of the magnetic probe ion.

Before the application of the Numerical Renormalization Group (NRG) to the Hamiltonian given by Eq. (1), we will introduce a basis given by two sets of s-wave operators, one sited at the magnetic probe and the other at the Anderson ion, which represent the new states of the conduction band on substitution of the operators $C_{\overrightarrow{k},\mu}$. In the present work the conduction band obeys the linear dispersion relation $\varepsilon_{\overrightarrow{k}} = v_F k$, where the energies and moments are measured in relation to the Fermi level and the units are taken so that $v_F = 1$. Considering the energy as an isotropic function of \overrightarrow{k} , i.e., $\varepsilon_{\overrightarrow{k}} = \varepsilon_{\left|\overrightarrow{k}\right|}$, the new operators are defined as

$$c_{\varepsilon\mu} = \frac{1}{\sqrt{\rho}} \sum_{\overrightarrow{k}} e^{i\overrightarrow{k} \cdot \overrightarrow{R}_f} \, \delta\left(\varepsilon - \varepsilon_k\right) c_{\overrightarrow{k},\mu} \tag{7}$$

$$d_{\varepsilon\mu} = \frac{1}{\sqrt{\rho}} \sum_{\overrightarrow{k}} e^{i\overrightarrow{k} \cdot \overrightarrow{R_p}} \delta(\varepsilon - \varepsilon_k) c_{\overrightarrow{k},\mu}, \tag{8}$$

where $c_{\varepsilon\mu}$ $(d_{\varepsilon\mu})$ is the operator which annihilates an electron at the s-wave state of the Anderson ion (magnetic probe), with energy ε and spin μ , sited at \overrightarrow{R}_f $(\overrightarrow{R_p})$, obeying the anticommutation relations

$$\begin{aligned}
\left\{c_{\varepsilon\mu}^{\dagger}, c_{\varepsilon'\mu'}\right\} &= \delta\left(\varepsilon - \varepsilon'\right) \delta_{\mu\mu'} \\
\left\{d_{\varepsilon\mu}^{\dagger}, d_{\varepsilon'\mu'}\right\} &= \delta\left(\varepsilon - \varepsilon'\right) \delta_{\mu\mu'}.
\end{aligned} \tag{9}$$

These operators do not form an orthogonal basis, since

$$\left\{c_{\varepsilon\mu}^{\dagger}, d_{\varepsilon'\mu'}\right\} = \frac{\sin\left(k_F R\right)}{\left(k_F R\right)} \delta\left(\varepsilon - \varepsilon'\right) \delta_{\mu\mu'},\tag{10}$$

where k_F is the Fermi momentum and $R = \left| \overrightarrow{R_f} - \overrightarrow{R_p} \right|$ is the distance between the Anderson ion and the magnetic probe. Using the Gram-Smidth orthogonalization process we define a new operator $\overline{c}_{\varepsilon\mu}$, orthogonal to $c_{\varepsilon\mu}$, obeying the standard anticommutation relation,

$$\bar{c}_{\varepsilon\mu} = \frac{1}{\sqrt{1 - W^2}} \left[d_{\varepsilon\mu} - W(R) c_{\varepsilon\mu} \right],\tag{11}$$

with $W(R) = \sin(k_F R) / (k_F R)$. To be used later, the operators $f_{0\mu z}$ and $g_{0\mu z}$ are defined as

$$f_{0\mu z} = \frac{1}{\sqrt{2}} \int_{-D}^{+D} d\varepsilon \rho^{1/2} c_{\varepsilon\mu}$$

$$g_{0\mu z} = \frac{1}{\sqrt{2}} \int_{-D}^{+D} d\varepsilon \rho^{1/2} \bar{c}_{\varepsilon\mu},$$
(12)

where ρ is the state density of the conduction band.

In terms of the operators $c_{\varepsilon\mu}$, $\bar{c}_{\varepsilon\mu}$, $f_{0\mu z}$ and $g_{0\mu z}$ the Hamiltonians H_{hib} , H_c and H_x are written as

$$H_{hib} = \sqrt{\frac{2\Gamma}{\pi\rho}} \left(f_{0z\mu}^{\dagger} c_{f\mu} + h.c. \right), \tag{13}$$

$$H_{cond} = \int_{-D}^{+D} d\varepsilon \, \varepsilon \left(c_{\varepsilon\mu}^{\dagger} c_{\varepsilon\mu} + \bar{c}_{\varepsilon\mu}^{\dagger} \bar{c}_{\varepsilon\mu} \right), \tag{14}$$

$$H_x = [A_1(R)g_{0z\uparrow}^{\dagger}g_{0z\downarrow} + A_2(R)(g_{0z\uparrow}^{\dagger}f_{0z\downarrow} + f_{0z\uparrow}^{\dagger}g_{0z\downarrow}) + A_3(R)f_{0z\uparrow}^{\dagger}f_{0z\downarrow}]\mathbf{I}_{-} + h.c,$$
(15)

where

$$A_{1}(R) = -2A (1 - W(R)^{2})$$

$$A_{2}(R) = -2AW(R) (1 - W(R)^{2})^{1/2}$$

$$A_{3}(R) = -2AW(R)^{2}$$
(16)

3 The Formalism

The conduction eigenstates of the Hamiltonian H_{cond} is represented by s-waves with two centers of symmetry, one sited at the Anderson ion (H_c) ,

$$H_c = \int_{-D}^{+D} d\varepsilon \, \varepsilon c_{\varepsilon\mu}^{\dagger} c_{\varepsilon\mu}$$

and the other at the magnetic probe $(H_{\bar{c}})$,

$$H_{\bar{c}} = \int_{-D}^{+D} d\varepsilon \; \varepsilon \bar{c}_{\varepsilon\mu}^{\dagger} \bar{c}_{\varepsilon\mu},$$

with $H_{cond} = H_c + H_{\overline{c}}$. Following Wilson [7], both the conduction bands, H_c and $H_{\overline{c}}$, are discretized as a function of the discretezation parameter $\Lambda > 1$, and the continue parameter $0 < z \le 1[10]$. The electronic states are written as a complete set of orthonormal functions in the domain (-D, D). For the extreme intervals, these function are given by

$$\Psi_{\ell}^{(\pm)}(\varepsilon) = \begin{cases}
\frac{1}{\left[D\left(1 - \Lambda^{-z}\right)\right]^{1/2}} e^{\pm i\omega\ell} \frac{\varepsilon}{D} & \text{for } \Lambda^{-z} < \pm \frac{\varepsilon}{D} < 1 \\
0 & \text{out side,}
\end{cases}$$
(17)

where \pm represent the positive or negative values of ε/D , ℓ is the Fourier harmonic index, which takes all integer values in the interval $(-\infty, +\infty)$, and $\omega = 2\pi/(1-\Lambda^{-z})$ is the fundamental frequency. In the internal intervals

$$\Psi_{m\ell}^{(\pm)}\left(\varepsilon\right) = \begin{cases} \frac{\Lambda^{\frac{m+z}{2}}}{\left[D\left(1-\Lambda^{-1}\right)\right]^{1/2}} e^{\pm i\omega_{m}\ell} \frac{\varepsilon}{D} & \text{for } \Lambda^{-(m+1+z)} < \pm \frac{\varepsilon}{D} < \Lambda^{-(m+z)} \\ 0 & \text{out side,} \end{cases}$$

where $m=0,1,2,\ldots$ label the descretization band intervals, and the parameter ω_m is the fundamental frequency of the *m-ésime* interval, given by $\omega_m=2\pi\Lambda^{m+z}/(1-\Lambda^{-1})$.

The operators $c_{\varepsilon\mu}$ and $\bar{c}_{\varepsilon\mu}$, are expanded in these basis as

$$c(\bar{c})_{\varepsilon\mu} = \sum_{\ell=-\infty}^{+\infty} \left[a(\bar{a})_{\ell\mu} \Psi_{\ell}^{(+)}(\varepsilon) + b(\bar{b})_{\ell\mu} \Psi_{\ell}^{(-)}(\varepsilon) \right] + \sum_{m=0}^{+\infty} \sum_{\ell=-\infty}^{+\infty} \left[a(\bar{a})_{m\ell\mu} \Psi_{m\ell}^{(+)}(\varepsilon) + b(\bar{b})_{m\ell\mu} \Psi_{m\ell}^{(-)}(\varepsilon) \right],$$

with

$$a(\bar{a})_{\ell\mu} = \int_{-D}^{+D} d\varepsilon \left[\Psi_{\ell}^{(+)}(\varepsilon) \right]^* c(\bar{c})_{\varepsilon\mu}; \qquad b(\bar{b})_{\ell\mu} = \int_{-D}^{+D} d\varepsilon \left[\Psi_{\ell}^{(-)}(\varepsilon) \right]^* c(\bar{c})_{\varepsilon\mu}$$

$$a(\bar{a})_{m\ell\mu} = \int_{-D}^{+D} d\varepsilon \left[\Psi_{m\ell}^{(+)}(\varepsilon) \right]^* c(\bar{c})_{\varepsilon\mu}; \qquad b(\bar{b})_{m\ell\mu} = \int_{-D}^{+D} d\varepsilon \left[\Psi_{m\ell}^{(-)}(\varepsilon) \right]^* c(\bar{c})_{\varepsilon\mu}, \tag{19}$$

where $a_{\ell\mu}$, $b_{\ell\mu}$, $a_{m\ell\mu}$, $b_{m\ell\mu}$ and $\bar{a}_{\ell\mu}$, $\bar{b}_{\ell\mu}$, $\bar{a}_{m\ell\mu}$, $\bar{b}_{m\ell\mu}$ form, respectively, complete sets of orthonormal operators obeying the standard anticommutation relations

$$\begin{cases}
a_{\ell\mu}, a_{\ell'\mu'}^{\dagger} \\
a_{m\ell\mu}, a_{m'\ell'\mu'}^{\dagger} \\
\delta_{m\ell\mu}, \bar{a}_{\ell'\mu'}^{\dagger} \\
\delta_{\ell\mu}, \bar{a}_{\ell'\mu'}^{\dagger} \\
\delta_{\ell\mu}, \bar{a}_{\ell'\mu'}^{\dagger} \\
\delta_{\ell\mu}, \bar{a}_{m'\ell'\mu'}^{\dagger} \\
\delta_{\ell\ell'}\delta_{\mu\mu'}
\end{cases} (20)$$

Replacing the expression for the oparator $a_{\varepsilon\mu}$ into the the expression for H_c 14 and eliminating the terms with $\ell \neq 0$, approach that was successfully used to calculate the magnetic susceptibility and the specific heat of the Kondo model [7, 9], the magnetic susceptibility [8] and the photoemission spectroscopy [10] of the Anderson model, H_c and $H_{\bar{c}}$ are written as

$$H_{c} = D \frac{1 + \Lambda^{-z}}{2} [(a_{\mu}^{\dagger} a_{\mu} - b_{\mu}^{\dagger} b_{\mu})$$

$$+ \sum_{m=0}^{+\infty} \Lambda^{-(m+z)} (a_{m\mu}^{\dagger} a_{m\mu} - b_{m\mu}^{\dagger} b_{m\mu})]$$

$$H_{\bar{c}} = D \frac{1 + \Lambda^{-z}}{2} [(\bar{a}_{\mu}^{\dagger} \bar{a}_{\mu} - \bar{b}_{\mu}^{\dagger} \bar{b}_{\mu})$$

$$+ \sum_{m=0}^{+\infty} \Lambda^{-(m+z)} (\bar{a}_{m\mu}^{\dagger} \bar{a}_{m\mu} - \bar{b}_{m\mu}^{\dagger} \bar{b}_{m\mu})]$$

where $a(\bar{a})_{0\mu} \equiv a(\bar{a})_{\mu}$, $b(\bar{b})_{0\mu} \equiv b(\bar{b})_{\mu}$, $a(\bar{a})_{m0\mu} \equiv a(\bar{a})_{m\mu}$ and $b(\bar{b})_{m0\mu} \equiv b(\bar{b})_{m\mu}$, for the conduction band electrons sited at the Anderson ion orbital (magnetic probe). The operators $f_{0z\mu}$ and $g_{0z\mu}$ of Eq.(12) are now written as

$$f_{0z\mu} = \left(\frac{1+\Lambda^{-z}}{2}\right)^{1/2} (a_{\mu} + b_{\mu}) + \left(\frac{1+\Lambda^{-1}}{2}\right)^{1/2} \sum_{m=0}^{+\infty} (a_{m\mu} + b_{m\mu}) e$$

$$g_{0z\mu} = \left(\frac{1+\Lambda^{-z}}{2}\right)^{1/2} (\bar{a}_{\mu} + \bar{b}_{\mu}) + \left(\frac{1+\Lambda^{-1}}{2}\right)^{1/2} \sum_{m=0}^{+\infty} (\bar{a}_{m\mu} + \bar{b}_{m\mu}),$$
(21)

obeying the orthonormalization condition

$$\begin{cases}
f_{0z\mu}, f_{0z\mu'}^{\dagger} \\
 = \delta_{\mu\mu'}
\end{cases}$$

$$\begin{cases}
g_{0z\mu}, g_{0z\mu'}^{\dagger} \\
 = \delta_{\mu\mu'}.
\end{cases}$$
(22)

The logarithmic discretization of the conduction band results in the definition of a basis of operators $\{a_{m\mu} (\bar{a}_{m\mu}), b_{m\mu} (\bar{b}_{m\mu})\}$, where $0 \leq m \leq \infty$, which is unsuitable for the numerical approach of the conduction electrons-Anderson ion interaction for all order of the hybridization Γ , since the Anderson ion orbital is coupled to all conduction states $a_{m\mu}$ and $b_{m\mu}$ via the operator $f_{0z\mu}$. Then a new basis $\{f_{nz\mu}, g_{nz\mu}\}$ will be defined, where each operator $f(g)_{nz\mu}$ is coupled only to the operators $f(g)_{(n\pm 1)z\mu}$ and solely the operator $f_{0z\mu}$ is coupled to the Anderson ion orbital [7].

Taking an unitary transformation of the set of operators $\{a(\bar{a})_{m\mu}, b(\bar{b})_{m\mu}\}$ to the new set of orthonormal operators $\{f(g)_{nz\mu}\}$, the conduction band Hamiltonians are given by

$$H_c = D \frac{1 + \Lambda^{-1}}{2} \sum_{n=0}^{\infty} \left(\varepsilon_n^z f_{nz\mu}^{\dagger} f_{(n+1)z\mu} + h.c. \right)$$
 (23)

$$H_{\bar{c}} = D \frac{1 + \Lambda^{-1}}{2} \sum_{n=0}^{\infty} (\varepsilon_n^z g_{nz\mu}^{\dagger} g_{(n+1)z\mu} + h.c.)$$
 (24)

where the parameter ε_n^z is numerically calculated. In the limit of large n, ε_n^z is approached by the asymptotic expression [10]

$$\varepsilon_n^z \cong \Lambda^{(1-z)-n/2},$$
 (25)

which for z = 1 recovers the Wilson expression [7].

The series in the Hamltonian H_c can be truncated without directly affect the interaction between the electrons of the Anderson ion orbital and the conduction band electrons. As the energy associated with the opertors $f_{nz\mu}$ and $g_{nz\mu}$, for large n, is of order of $\Lambda^{(1-z)-n/2}$, one can choose a n=N sufficient large so that this quantity becomes very small as compared with the energy scale relevant to the problem which is defined by the temperature,

$$D\frac{1+\Lambda^{-1}}{2}\Lambda^{(1-z)-N/2} \ll k_B T.$$
 (26)

The truncated Hamiltonian H_c and $H_{\overline{c}}$ are written as

$$H_{c} = D \frac{1 + \Lambda^{-1}}{2} \sum_{n=0}^{N-1} \varepsilon_{n}^{z} \left(f_{nz\mu}^{\dagger} f_{(n+1)z\mu} + h.c. \right)$$

$$H_{\bar{c}} = D \frac{1 + \Lambda^{-1}}{2} \sum_{n=0}^{N-1} \varepsilon_{n}^{z} \left(g_{nz\mu}^{\dagger} g_{(n+1)z\mu} + h.c. \right)$$

It is interesting to be observed that the truncation of the series in the Hamiltonians H_c doesn't affect the energy of the Anderson ion orbital, since the coupling of the conduction electrons with the electrons of this orbital is only via the operator $f_{0z\mu}$ of the basis $\{f_{nz\mu}\}$.

The Hamiltonian H (Eq.(1)), in terms of the operators of the basis $\{f_{nz\mu}, g_{nz\mu}\}$, can be written as

$$H = H_A + H_{\bar{c}}$$

$$H_A = D \left\{ \frac{1 + \Lambda^{-1}}{2} \sum_{n=0}^{N-1} \varepsilon_n^z \left(f_{nz\mu}^{\dagger} f_{(n+1)z\mu} + h.c. \right) + \frac{\varepsilon_f}{D} c_{f\mu}^{\dagger} c_{f\mu} + \frac{U}{D} c_{f\uparrow}^{\dagger} c_{f\uparrow} c_{f\downarrow} c_{f\downarrow} + \sqrt{\frac{2\Gamma}{\pi D}} \left(f_{0z\mu}^{\dagger} c_{f\mu} + h.c \right) \right\}$$

where the state density of the conduction band $\rho = 1/D$. For a better interpretation of the results, we define H_A^N and $H_{\bar{c}}^N$ as the Hamiltonian H_A and $H_{\bar{c}}$ divided by $D(1 + \Lambda^{-1})\Lambda^{-(N-1)/2}/2$, respectively, so that the smallest energy scale associated to the operator $f_{(N-1)z\mu}^{\dagger}f_{N)z\mu} + f_{Nz\mu}^{\dagger}f_{(N-1)z\mu}$ and

 $g^{\dagger}_{(N-1)z\mu}g_{N)z\mu}+g^{\dagger}_{Nz\mu}g_{(N-1)z\mu}$ be on the order of unity:

$$H^{N} = H_{A}^{N} + H_{\bar{c}}^{N}$$

$$H_{A}^{N} = \Lambda^{-(N-1)/2} \left\{ \sum_{n=0}^{N-1} \varepsilon_{n}^{z} \left(f_{nz\mu}^{\dagger} f_{(n+1)z\mu} + g_{nz\mu}^{\dagger} g_{(n+1)z\mu} + h.c. \right) + \tilde{\varepsilon}_{f} c_{f\mu}^{\dagger} c_{f\mu} + \tilde{U} c_{f\uparrow\uparrow}^{\dagger} c_{f\uparrow} c_{f\downarrow}^{\dagger} c_{f\downarrow} + \Gamma^{1/2} \left(f_{0z\mu}^{\dagger} c_{f\mu} + h.c \right) \right\}$$

$$H_{\bar{c}}^{N} = \Lambda^{-(N-1)/2} \sum_{n=0}^{N-1} \varepsilon_{n}^{z} \left(g_{nz\mu}^{\dagger} g_{(n+1)z\mu} + h.c. \right)$$

$$(27)$$

where

$$\widetilde{\varepsilon}_{f} = \frac{2}{1 + \Lambda^{-1}} \frac{\varepsilon_{f}}{D}$$

$$\widetilde{U} = \frac{2}{1 + \Lambda^{-1}} \frac{U}{D}$$

$$\widetilde{\Gamma} = \left(\frac{2}{1 + \Lambda^{-1}}\right)^{2} \frac{2\Gamma}{\pi D}.$$
(28)

As $\{H_A^N, H_{\overline{c}}^N\} = 0$, the Hamiltonians H_A^N and $H_{\overline{c}}^N$ are diagonalized separately and the eigenstates of H^N are direct products of the eigenstates of H_A^N and $H_{\overline{c}}^N$. The diagonalization of the Hamiltonians H_A^N and $H_{\overline{c}}^N$ are performed iteractively in subspaces of the same charge and spin (Q,S,S_z) . The diagonalization process of H_A^N begins with the diagonalization of the Anderson ion Hamiltonian

$$H_A^{-1} = \frac{\widetilde{\varepsilon}_f}{\Lambda} c_{f\mu}^{\dagger} c_{f\mu} + \frac{\widetilde{U}}{\Lambda} c_{f\uparrow}^{\dagger} c_{f\uparrow} c_{f\uparrow} c_{f\downarrow}^{\dagger} c_{f\downarrow}. \tag{29}$$

In the second step we add the operator $f_{0z\mu}$ and diagonalize the Hamiltonian

$$H_A^0 = \frac{H_A^{-1}}{\sqrt{\Lambda}} + \frac{\widetilde{\Gamma}^{1/2}}{\sqrt{\Lambda}} \left(f_{0z\mu}^{\dagger} c_{f\mu} + c_{f\mu}^{\dagger} f_{0z\mu} \right)$$
 (30)

in relation to a basis formed by the eigenstates of the Hamiltonian of the first step (H_A^{-1}) and the states that are constructed by the operators $f_{0z\uparrow}^{\dagger}$, $f_{0z\downarrow}^{\dagger}$ and $f_{0z\uparrow}^{\dagger}f_{0z\downarrow}^{\dagger}$ applied to the eigenstates of H_A^{-1} . Following this procedure, the Hamiltonian H_A^{N+1} is diagonalized in relation to a basis formed by the eigenstates of H_A^N and the states given by the operators $f_{(N+1)z\uparrow}^{\dagger}$, $f_{(N+1)z\downarrow}^{\dagger}$ and $f_{(N+1)z\uparrow}^{\dagger}f_{(N+1)z\downarrow}^{\dagger}$ applied to those eigenstates. The same procedure of iteractive diagonalization is used to diagonalize the Hamiltonian $H_{\bar{c}}^{N}$.

The ralaxation time $T_1(z)$ is written as the Fermi golden rule [13]:

$$\frac{1}{\mathrm{T}_{1}\left(z\right)} = \frac{4\pi}{h} \sum_{I,F} P_{I}\left(z\right) \left|\left\langle I\left(z\right)\right| H_{x} \left|F\left(z\right)\right\rangle\right|^{2} \delta\left(E_{I}\left(z\right) - E_{F}\left(z\right)\right),$$

where

$$P_{I}(z) = \frac{e^{-\beta E_{I}(z)}}{\sum_{I} e^{-\beta E_{I}(z)}},$$

is the statistical Boltzmann weight, $\beta = 1/k_B T$, k_B is the Boltzmann constant, T is the temperature and $|I(z)\rangle$ and $|F(z)\rangle$ are the initial and final many-particles states of the Hamiltonian H, with energy $E_I(z)$ and $E_F(z)$, respectively. In terms of the eigenstates of the Hamiltonian given by Eq. (27), the ralaxation time $T_1(z)$ is written as

$$\frac{1}{\mathrm{T}_{1}(z)} = \frac{4\pi}{h} D\left(\frac{1+\Lambda^{-1}}{2}\right) \Lambda^{-(N-1)/2} \times \sum_{I,F} e^{-\beta_{N}\Lambda^{(z-1)}E_{IN}(z)} \left| \langle I(z)| H_{x}^{N} | F(z) \rangle \right|^{2} \delta\left(E_{IN}(z) - E_{FN}(z)\right)}{\sum_{I} e^{-\beta_{N}\Lambda^{(z-1)}E_{IN}(z)}}, \tag{31}$$

where

$$\beta_N = \left(\frac{1+\Lambda^{-1}}{2}\right) \Lambda^{-(N-1)/2} \frac{D}{k_B T} \Lambda^{(1-z)}.$$

In the iteractive process we take β as a constant, $\beta_N = \bar{\beta}$, with $\bar{\beta} < 1$, and T as a function of N (T_N) , according to Wilson method to calcuate the magnetic susceptibility of the Kondo model [7],

$$k_B T_N(z) = \left(\frac{1+\Lambda^{-1}}{2}\right) \Lambda^{-(N-1)/2} \frac{D}{\overline{\beta}} \Lambda^{(1-z)}.$$

As a consequence of the logarithmic discretization of the conduction band, Eq.(31) gives discrete lines centered at the energy $E_{IN}(z) - E_{FN}(z)$. To transform these discrete lines in a continuum spectrum the Dirac delta function propriety

$$\delta\left(E_{IN}\left(z\right) - E_{FN}\left(z\right)\right) = \sum_{z_0} \frac{\delta\left(z - z_0\right)}{\left|\frac{d}{dz}\left(E_{IN}\left(z\right) - E_{FN}\left(z\right)\right)\right|_{z = z_0}},$$

was used where z_0 is the roots of the function $f(z_0) = E_{IN}(z_0) - E_{FN}(z_0)$, and average $\frac{1}{T_1(z)}$ over z inside the interval $(z^*, z^* + 1)$, with $z^* \in (0, 1)$,

$$\frac{1}{T_{1}} = \frac{4\pi}{h} k_{B} \bar{\beta} \sum_{z_{0}} \Lambda^{(z_{0}-1)} T_{N}(z_{0}) \sum_{I,F} \bar{P}_{I}(z_{0}) \frac{\left| \langle I(z_{0}) | H_{x}^{N} | F(z_{0}) \rangle \right|^{2}}{\left| \frac{d}{dz} \left(E_{IN}(z) - E_{FN}(z) \right) \right|_{z=z_{0}}},$$
(32)

with

$$\bar{P}_{I}(z_{0}) = \frac{e^{-\bar{\beta}\Lambda^{(z_{0}-1)}E_{IN}(z_{0})}}{\sum_{I} e^{-\bar{\beta}\Lambda^{(z_{0}-1)}E_{IN}(z_{0})}}.$$

4 Results and discussion

In this section we have shown the results of the relaxation time $1/T_1$ of the magnetic probe that interacts with the electrons of the Anderson ion via a RKKY interaction given by Eq. (15). In this discussion the coupling constant A between the magnetic probe and the conduction electrons will be taken as $(h/(4\pi k_B \rho^2)^{1/2})$.

We begin by verifying the accuracy of our numerical results, comparing the numerical renormalization group results for U=0 with the analytical solution [3, 14]. In Fig.(1) we present $1/(T_1T)$ as a function of the temperature T. For $k_BT\gg -\varepsilon_f$, $1/(T_1T)$ tends for one, as is expected for pure metal. The transition from the valence fluctuation to the doubly occupied orbital regime occurs near the temperature in the order of $\Delta=-\varepsilon_f$, where $1/(T_1T)$ presents a minimum due to the reduction of the density of state of the conduction band close to the Anderson ion. For $k_BT\ll -\varepsilon_f$, $1/(T_1T)$ tends for a constant value of 0.9846 (traced line), in accordance wih the analytical result of 0.9803 (full line) obtained from the equation [14]

$$\left(\frac{h}{4\pi\rho^2 A^2 k_B}\right) \frac{1}{T \ \mathrm{T_1}} = \left(\frac{\Delta^2}{\Delta^2 + \Gamma^2}\right)^2,$$

with an error lower than 1%.

The analysis of the results will be carried out for $U \neq 0$ and two regimes of the parameter space of the Anderson model: the valence fluctuation and the singly occupied orbital. We separate the results for W=1 (R=0), with the magnetic probe close to the Anderson ion site, and $W \neq 1 (R>0)$, with the magnetic probe sited at a distance R from the Anderson ion.

The valence fluctuation regime occurs for $-1 < \Gamma/\Delta < 1$ and $\varepsilon_f \gg \Gamma$. In this case, the configurations of doubly and singly occupied orbital are mixed and the number of particle in the fundamental state is in the interval $1 < n_f < 2$. In Fig. (2) we show $1/(T_1T)$ for $\varepsilon_f = -0.01D$, $\Gamma = 0.001D$ and two values of Δ (0.0005D and 0.0007D), for W = 1(R = 0), i.e., with the magnetic probe close to the Anderson ion site. For $k_BT \gg -\varepsilon_f$, $-\Delta$ all the configurations ($n_f = 0, 1, 2$) are thermically populated and $1/(T_1T)$ tends to one, as in pure metal. Lowering T, for $T \approx \Delta$, the Anderson ion orbital is in the valence fluctuation regime, where the coupling between the two configurations ($n_f = 1$ and $n_f = 2$) reduces the number of conduction states around the magnetic probe site, with the corresponding reduction in $1/(T_1T)$. For $k_BT \ll \Delta$, the Anderson ion orbital is strongly coupled to the conduction electrons and the system behaves as a Fermi sea, with $1/(T_1T)$ lower than one. For low T, $1/(T_1T)$ increases with the increasing of Δ . For high Δ , the contribution of the configuration $n_f = 1$

for the fundamental state increases and the Anderson ion orbital behaves as a Kondo impurity, which will be discussed as follows.

The Anderson ion orbital is singly occupied when Δ , $-\varepsilon_f \gg \Gamma$. The interaction U between the electrons inside this orbital increases the energy of the configuration $n_f = 2$, so that in the fundamental state the Anderson ion orbital is in the configuration $n_f = 1$. At low $T(k_B T \ll \Gamma)$ the electrons of the Anderson ion orbital is strongly coupled to the electrons of the conduction band, with virtual transition between the configuration $n_f = 1$ and $n_f = 2$, with the additional electron coming from the conduction band. The spin states $(n_f = 1, \mu = -1/2 \text{ and } n_f = 1, \mu = 1/2)$ are doubly degenerated, so that there is an effective antiferromagnetic exchange interaction between the electrons of the Anderson ion orbital and the conduction electrons, breaking the degeneracy of the configurations $\mu = -1/2$ and $\mu = 1/2$, arising the well known Kondo effect. From the coupling between these configurations emerge a singlet and a triplet state, with an energy separation k_BT_k , where T_k is known as the Kondo temperature. A measure with characteristic time $\gtrsim \hbar/k_BT_k$ can detect the spin inversion of a electron of the Anderson ion orbital, which occurs in this period of time. In order for the total magnetic moment of the fundamental state to remain zero, the electrons of the conduction band go along with the spin inversion of the electron of the Anderson ion orbital, so that the electrons with energy the order of k_BT stay a long time around these orbital, increasing the scattering of the conduction electrons, with an increasing in the spin relaxation rate. In Fig.(3) we present $1/T_1$ as a function of the temperature for the parameters of the model representing the Kondo regime, $\varepsilon_f = 0.1D$, $\Gamma = 0.011D$ and three values for Δ (0.05D (A), 0.07D (B), 0.09D (C)), considering W = 1(R = 0), the magnetic probe close to the Anderson ion site. The peaks occur around Γ_k (the Kondo width), which is given by

$$\Gamma_k = \frac{T_k}{2\pi \times 0.103},\tag{33}$$

and takes the values $\Gamma_k = 1.26 \times 10^{-4} D$ (A), $4.01 \times 10^{-5} D$ (B) and $1.65 \times 10^{-5} D$ (C). The Kondo temperature T_k is calculated from the magnetic susceptibility results [7], using the K. G. Wilson criterion

$$\frac{\chi(T)}{(\mathbf{g}\mu_B)^2} \cong \frac{0,10}{k_B T_K} \text{ for } T \ll T_K, \tag{34}$$

where $\chi\left(T\right)$ is the magnetic susceptibility, \mathbf{g} is the Landé factor and μ_{B} Bohr magneton.

For low temperature, the heavy Fermi liquid behavior is better observed in Fig. (4), where we show $1/(T_1T)$ as a function of T, using the same parameters of Fig.(3). For $k_BT \ll T_k$, $1/(T_1T)$ is drastically enhanced as compared with the normal metal results, and increases as the Kondo temperature T_k decreases.

The thermodynamics proprieties of the Anderson model in the Kondo regime, like the magnetic susceptibility, are characterized by a universal behavior [8] when the temperature is scaled by the Kondo temperature T_k . This universal

behavior is also observed in the electron spin resonance when the spin relaxation rate is multiplied by the temperature. In Fig. (5) we show the universality of T/T_1 in the Kondo regime for $\varepsilon_f = 0.1D$, $\Gamma = 0.001D$ and three values for Δ (0.05D (A), 0.07D (B), 0.09D (C)), considering W = 1(R = 0). The universality remains for temperatures the order of $100\Gamma_k$.

In Fig. (6) we compare the spin relaxation time $1/T_1$ with the magnetic susceptibility χ of the Anderson ion orbital. For temperatures lower then T_k the spin relaxation rate $1/T_1$ is proportional to χT , in qualitative agreement with the experimental results of Coldea *et al.* [15] for Kondo lattice.

Increasing the distance between the Anderson ion orbital and the magnetic probe, $W \neq 1(R>0)$, decreases the contributions of the term $A_1(R) g_{0z\mu}^\dagger g_{0z\mu}$, where $A_1 \propto (1-W(R)^2)$, $A_3 \propto W(R)^2$ and $W(R) = \sin(kR)/(kR)$. On the other hand, the contribution of the term $A_2(R)(f_{0z\mu}^\dagger g_{0\mu} + g_{0z\mu}^\dagger f_{0z\mu})$, where $A_2 \propto W(R)\sqrt{(1-W(R)^2)}$, increases with the reduction of W(R) until reaching its maximum value $W(R) = \sqrt{2}/2$, after which it decreases until zero at the limit $R \to \infty$. In this limit only the term $A_1(R)g_{0z\mu}^\dagger g_{0z\mu}$ survives , so that the spin relaxation rate is equal to a pure metal. In Fig.(7) we present the spin relaxation rate $1/T_1$ for W(R) = 1.0, 0.7, 0.5, and 0.3, with the parameter of the Anderson model given by $\varepsilon_f = -0.1D$, $\Gamma = 0.011D$ and $\Delta = 0.05D$. The Kondo peak, which is sited at the temperature the order of the Kondo width $\Gamma_k = 1.258 \times 10^{-4}D$, decreases with the increasing of the distance R between the Anderson ion and the magnetic probe. The inset of the Fig.(7) shows that the Kondo effect remains even for large distances, being eliminated only in the limit $R \to \infty$ $(W \to 0)$.

The Fermi liquid behavior is analyzed in Fig. (8), where we present $\gamma =$ $1/(T_1T)$ as a function of Δ/Γ at very low temperature, taking $\Gamma = 0.011D$, $\varepsilon_f =$ -0.10D and four values W (1.0, 0.7, 0.5 and 0.3). For a fixed value of ε_f , the ratio Δ/Γ varies continuously from $\Delta \ll -\Gamma$ to $\Delta \gg \Gamma$, crossing three regimes: the regime of Anderson ion orbital doubly occupied ($\Delta \ll -\Gamma$), the intermediate valence regime $(-\Gamma < \Delta < \Gamma)$, and the Kondo regime $(\Delta \gg \Gamma)$. For $\Delta \ll$ $-\Gamma$ the Anderson ion orbital is doubly occupied and γ is up bounded by one. By increasing Δ the energy of the configuration with doubly occupied orbital approaches the energy of the configuration with a singly occupied orbital, and γ decreases monotonically to zero, where these two configurations are degenerated. For $\Delta \gg \Gamma$, in the Kondo regime, the single orbital configuration becomes dominant and γ suffers a huge increase. For $-\Gamma < \Delta < \Gamma$, in the intermediate valence regime, depending on the ratio Δ/Γ , the constant γ can be smaller or greater than one, so that T_1^{-1} can be reduced or enhanced in relation to a pure metal relaxation rate. This is in contrast with the particular case of Coulomb interaction U = 0 used by Gambke at al [3] to analyze intermediate valence compound, in which γ is always reduced in relation to the Korringa relaxation rate of pure metal.

5 Conclusion

We have calculated the relaxation rate $1/T_1$ of a magnetic probe sited at a distance R from the impurity of the spin degenerated Anderson model, using numerical renormalization group formalism. The numerical result is in very good agreement with the analytical result for U=0. In the valence fluctuation regime the curve $\gamma=1/(TT_1)$ presents a depression at temperature the order of Δ , which is the difference between the energy of the configurations $n_f=1$ and $n_f=2$, and behaves as a Fermi liquid for very low temperature, augmenting γ as Δ increases.

In the Kondo regime $1/T_1$ presents a peak at the Kondo width Γ_k , which height increases as Γ_k decreases. For temperature much lower then Γ_k the system behaves as a Fermi liquid, presenting a dramatic enhancement in the relaxation rate. The product of the temperature by the relaxation rate (T/T_1) as function of the temperature scaled by Γ_k obeys an universal function, even for temperatures of the order of $100\Gamma_k$. For temperature lower then Γ_k , the relaxation rate $1/T_1$ is proportional to the product of the temperature by the magnetic susceptibility $(T\chi)$. Increasing the distance R between the magnetic probe and the Anderson impurity, the peak at Γ_k decreases until it disappears at $R \to \infty$. For very low temperatures, $\gamma = 1/(TT_1)$ as a function of Δ/Γ approaches to one in the region where the Anderson impurity is doubly occupied $(\Delta/\Gamma < 1)$, presents a minimum in the region of valence fluctuation regime $(-1 < \Delta/\Gamma < 1)$, and is drastically enhanced in the region of the Kondo regime $(\Delta/\Gamma > 1)$.

FIGURE CAPTIONS

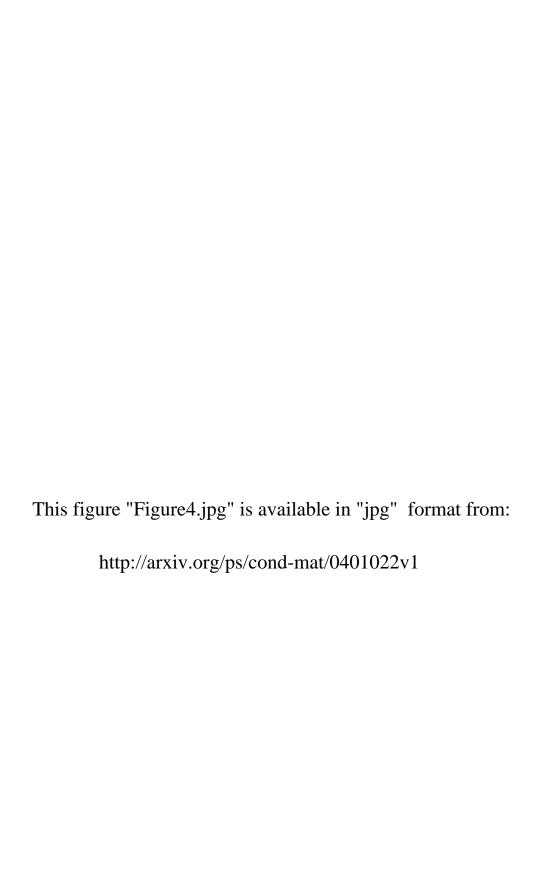
- Fig. 1. Numerical renormalization group result for $1/(T_1T)$ as a function of the temperature (full line) for U=0 and R=0, as compared with the analytical result (traced line) [12], with a lower than 1% error.
- Fig. 2. The rate $\gamma = 1/(TT_1)$ as a function of the temperature for the valence fluctuation regime and R = 0. For $k_B T \gg -\varepsilon_f$, all the Anderson ion states are thermically accessible and the system behaves as a pure metal; for $k_B T \approx \Delta$, $1/(TT_1)$ has a minimum due to the reduction in the density of states around the magnetic probe; for $k_B T \ll \Gamma$, $1/(TT_1)$ is constant and increases with Δ .
- Fig. 3. The spin relaxation rate T_1^{-1} as a function of the temperature for three sets of parameters of the Anderson model, taking fixed ε_f and Γ , and varying Δ . The curves present a peak at the Kondo width $\Gamma_k = 1.26 \times 10^{-4} D$ (curve A), $\Gamma_k = 4.01 \times 10^{-5} D$ (curve B) and $\Gamma_k = 1.65 \times 10^{-5} D$ (curve C), which are marked in the temperature axis. Γ_k was obtained from the magnetic susceptibility, as given by Eq. (39), using the Wilson relation $\Gamma_k = T_k/(2\pi \times 0.103)$. The height of the peak grows with the reduction of the Kondo temperature.
- Fig. 4. The rate $\gamma = 1/(TT_1)$ as a function of the temperature for the same parameters of Fig.(3). For high T, the system behaves as a pure metal; lowering the temperature, the curves present a minimum, associated with the valence fluctuation regime; for $T \ll \Gamma_k$, the γ is enhanced in the Kondo regime, and the system behaves as a heavy Fermi liquid.
- Fig. 5. In the Kondo regime, T/T_1 behaves as a universal function of the T/Γ_k . The figure presents three sets of Anderson model parameter in the Kondo regime, and the universality behavior of T/T_1 remains until temperatures of the order of $100\Gamma_k$.
- Fig. 6. In the Kondo regime, the spin relaxation rate T_1^{-1} is proportional to χT . The figure presents T_1^{-1} and χT for the same set of parameters of the Anderson model, in the Kondo regime, where T_1^{-1} is proportional to χT for temperature lower than the Kondo temperature (marked in the temperature axis).
- Fig. 7. Spin relaxation rate T_1^{-1} as a function of the temperature for four distances R between the Anderson ion and the magnetic probe, corresponding to W = 1 (the magnetic probe very close to the Anderson ion), and W = 0.7, 0.5, and 0.3. The Kondo peak decreases with the distance R. Even for long distance (curve D), the peak survives, as is shown in the inset.
- Fig. 8. The rate $\gamma=1/(TT_1)$ as a function of Δ/Γ , for very low temperature and deferent distances between the Anderson ion and the magnetic probe. For $\Delta/\Gamma\ll-1$, the Anderson ion is doubly occupied, for $-1<\Delta/\Gamma<1$ is in the intermediate valence regime, and for $\Delta/\Gamma\gg1$, is in the Kondo regime. The curves are lower than one for the Anderson ion in the doubly occupied regime, present a minimum in the valence fluctuation regime, and are enhanced in the Kondo regime.

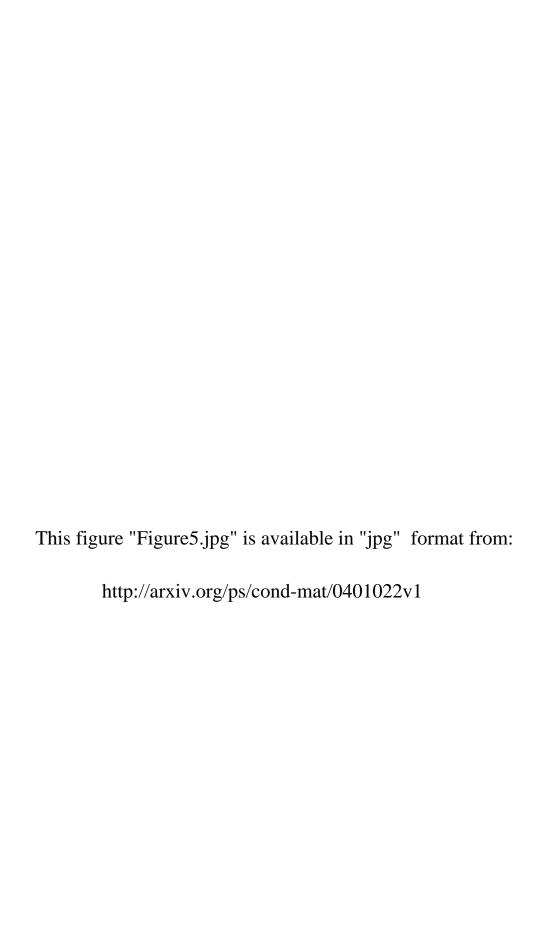
References

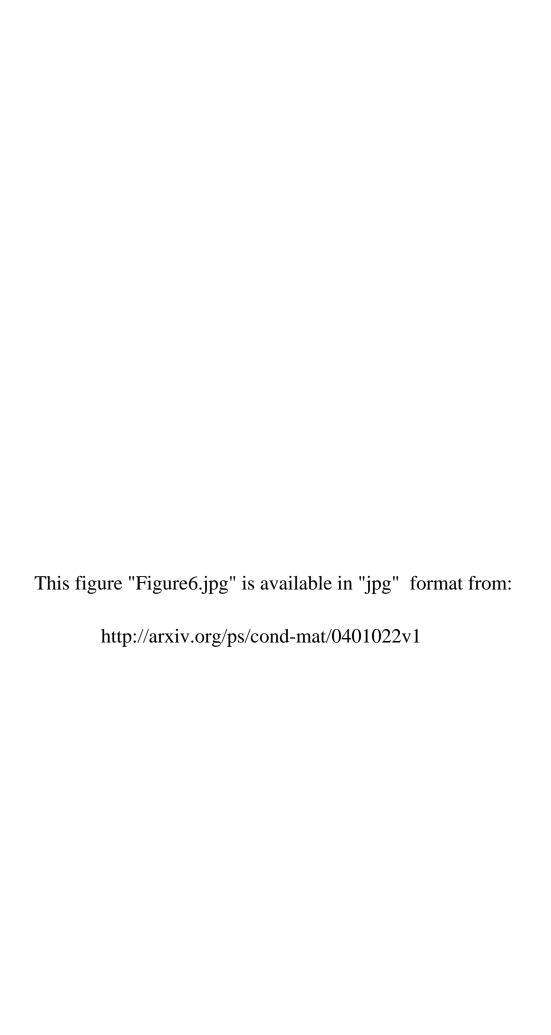
- [1] P. W. Anderson, Phys. Rev. **124**, 442 (1961).
- [2] H.-A, Krug von Nidda, A. Schutz, M. Heil, B. Elschner and A. Loidl, Phys. Rev. B 57, 14344 (1998).
- [3] T. Gambke, B. Elschner and L. L. Hirst, Phys. Rev. Lett. 40, 1290 (1978).
- [4] G. Heirinch and A. Mayer, Solid State Commun. 24, 1 (1977).
- [5] G. E. Barberis, D. Davidov, C. Rettori, J. P. Donoso, I. To rriani and F. C. G. Gandra, Phys. Rev. Lett. 45, 1966 (1980).
- [6] C. Rettori, S. B. Oseroff, D. Rao, P. G. Pagliuso, G. E. Barberis, J. Sarrao, Z. Fisk and M. Hundley, Phys. Rev. B 55, 1016 (1997).
- [7] K. G. Wilson, Rev. Mod. Phys. 47, 773 (1975).
- [8] Krishna-Murty, H. R., Wilkins, J. W. and Wilson, K. G.; Phys. Rev. B 21, 1003 (1980); Krishna-Murty, H. R., Wilkins, J. W. e Wilson, K. G.; Phys. Rev. B 21, 1044 (1980).
- [9] L. N. Oliveira and J. W. Wilkins, Phys. Rev. Lett. 47, 1553 (1981).
- [10] H. O. Frota and L. N. Oliveira, Phys. Rev. B 33, 7871 (1986).
- [11] M. A. Yoshida, M. A. Whitaker, L. N. Oliveira, Phys. Rev. B 41, 9403 (1990).
- [12] M. A. Ruderman and C. Kittel, Phys. Rev. 96, 99 (1954); T. Kasuya, Prog. Theor. Phys. 16, 45 (1956); K. Yoshida; Phys. Rev. 106, 893 (1957).
- [13] J. Winter, Magnetic Resonance in Metals (Oxford University Press. London, 1971).
- [14] J. W. M. Pinto and H. O. Frota, Phys. Rev. B 64, 92404 (2001).
- [15] M. Coldea, H. Schaeffer, V. Weissenberger, and B. Elschener, Z. Phys. B Condensed Matter 68, 25 (1987).

This figure "Figure1.JPG" is available in "JPG" format from: http://arxiv.org/ps/cond-mat/0401022v1

This figure "Figure2.jpg" is available in "jpg" format from: http://arxiv.org/ps/cond-mat/0401022v1 This figure "Figure3.jpg" is available in "jpg" format from: http://arxiv.org/ps/cond-mat/0401022v1







This figure "Figure7.jpg" is available in "jpg" format from: http://arxiv.org/ps/cond-mat/0401022v1

